

Density Matching for Microencapsulation of Field Responsive Suspensions of Non-Brownian Microparticles

Samuel R. Wilson-Whitford,* Jinghui Gao, and James F. Gilchrist*



Cite This: *J. Phys. Chem. B* 2024, 128, 6394–6399



Read Online

ACCESS |



Metrics & More

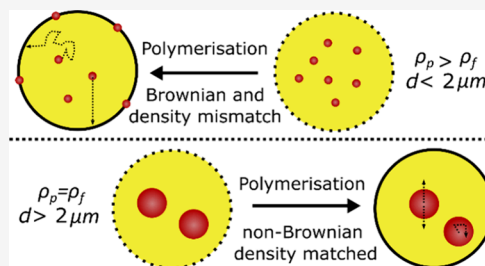


Article Recommendations



Supporting Information

ABSTRACT: When forming composite microcapsules through the emulsification of a dispersed phase laden with microparticles, one will find that the microparticles become irreversibly embedded in the resulting microcapsule membrane. This phenomenon, known as Pickering stabilization, is detrimental when the end function of the microcapsules relies on the mobility of encapsulated microparticles within the capsule core. In this work, a robust microencapsulation route using density matching of non-Brownian microparticles in a binary solvent is shown to easily and effectively encapsulate particles, with >90% of particles retaining mobility within the microcapsules, without the necessity for prior chemical/physical modifications to the microparticles. This is proposed as a generalized method to be used for all manner of particle chemistries, shapes, and sizes.



INTRODUCTION

Microcapsules containing microparticles, either at the interface or contained within the core of capsules, are a type of composite material capable of combining the desirable properties of their component materials. Encapsulated particles can have any number of chemistries, with the microcapsule itself providing either a structural template or compartmentalization vessel for what are usually expensive microparticle additives. Combinations of capsules and particles can be used to control capsule structural properties¹ and release dynamics,^{2–4} or used in analytics,⁵ as microreactors,⁶ responsive systems,⁷ and electrochemical and absorption micromaterials,^{8–10} in a wide variety of pharmaceutical, environmental, and energy applications.

Typically, emulsification in the presence of microscale particles can result in adsorption of particles to the droplet interface, in a process called Pickering stabilization.^{11–13} There is a significant energetic advantage to solid particles occupying the interface.^{14,15} The presence of particles in the dispersed phase during microencapsulation has a tendency to exacerbate this phenomenon, with particles almost instantaneously stabilizing the interface, even under laminar conditions in microfluidic experiments.¹⁶ Although there are a wealth of applications for particle-stabilized/armored capsules, there are of course examples where the desired result is for particles to be freely suspended or mobile inside the core of microcapsules.

One of the most convenient and intuitive approaches to minimize particle adsorption to the interface is to significantly restrict the Brownian motion of the encapsulant particles during the microencapsulation process. This is done typically through control of the rheology of the core.^{17–20} However, in most cases, the gelation of the core will be irreversible and will permanently restrict the mobility of encapsulant particles, which in the context of this discussion is counterproductive. Likewise, yield

stress and viscoelastic fluids increase complexity with regard to scale-up. Lim and Moss demonstrated a series of techniques for encapsulating biologicals using an aqueous reliquification approach making use of ionic cross-linking and chelation agents.^{21–23} Previously, the use of a yield stress core material that was sufficiently weak as to yield under externally imparted forces, facilitating particle motion, was demonstrated for suspensions of encapsulated particles.²⁴

Generation of particles *in situ* within the core of capsules has been shown using variations on emulsion polymerization^{25–29} and template-free approaches,^{30,31} but these approaches are often limited to producing capsules where the core particles and capsule wall are made of the same material. Alternatively, layer-by-layer approaches in which the encapsulant particle is first coated in a sacrificial layer, which can later be removed following shell formation,^{32–37} are capable of producing highly monodisperse materials, at the cost of being synthetically laborious. Additionally, there are approaches that rely on utilizing complementary surface energies or chemical modification of particles.^{38–40} In circumstances where the experimental and/or product parameters are strict, the use of surface modification of particles is an effective methodology for encapsulating mobile particles. However, each new formulation will require a similar degree of experimentation and optimization.

Received: April 8, 2024

Revised: May 11, 2024

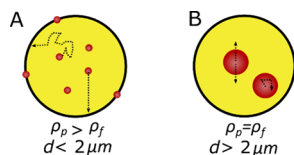
Accepted: May 15, 2024

Published: May 23, 2024



Additionally, it is not always practical or possible to modify the surface properties and wetting of the particles that will be encapsulated or to conduct extensive solvent searches for surface energy matching. Likewise, the solidification of cores or the modification of the core viscosity can also be restrictive to applications. Therefore, there is a need for a direct, easily scalable approach. This can be especially relevant for industrial applications where the synthesis of custom particles can be prohibitively expensive. Here, it is proposed that provided a particle is neutrally buoyant, preventing sedimentation, and sufficiently large so that Brownian diffusion is insignificant, the time for particle migration to the interface will be greater than the time of membrane polymerization, therefore maintaining a high proportion of mobile particles in the compartmentalized suspensions (Scheme 1). This method is a generalized synthetic

Scheme 1. Schematic of (A) Particle Adsorption to Microcapsule Membranes in a Typical Microencapsulation of Suspended Particles. (B) Proposed Microencapsulation of Density Matched Non-Brownian Microparticles^a



^aIn the scheme, d refers to the particle diameter, ρ_p is the particle density, and ρ_f is the fluid density.

approach that is applicable to a range of particle sizes, generally $>2 \mu\text{m}$ diameter, shapes, and chemistries of variable wetting and having moderate density.

METHODS

Janus Particle Synthesis. The synthetic method for preparation of the $50 \mu\text{m}$ Janus particles used in this article is previously outlined in full in another publication.⁴¹ In short, monolayers of $\sim 45 \mu\text{m}$ poly(methyl methacrylate) particles were prepared by using an automated Langmuir–Blodgett (ALB) method.⁴² These monolayers were coated with iron, which in turn oxidized to iron oxide, via treatment with physical vapor deposition (PVD). The resulting Janus particles were removed from the substrate in ethanol using sonication and subsequently dried.

Microcapsule Synthesis. The full list of experimental compositions is given in Table 1. An example synthesis for sample 3 is given here: In a 250 mL beaker, a 2 wt % solution of Mowiol 8-88 PVA was prepared and heated to $45 \text{ }^\circ\text{C}$. An impeller stirrer was positioned centrally in the beaker, and the solution was stirred at 450 rpm. In a 20 mL glass vial, 7.5 mL of

the binary solvent was prepared by using 3.00 mL of dodecane and 6.00 g of halocarbon 0.8 oil. To this binary solvent 0.018 g of Span 80, 0.089 g of Janus particles, and $625 \mu\text{L}$ of isophorone diisocyanate were added. The density of the dispersed phase was adjusted dropwise with halocarbon or dodecane until Janus particles were neutrally buoyant. The suspension was sonicated for 5 min and was then quickly added into the stirring continuous phase and left to stir at 500 rpm for 20 s. Immediately following this, the stir speed was adjusted to 150 rpm, and 3 mL of 10 w/w diethylene triamine solution was added dropwise over 30 s. The reaction was left for 4 h, resulting in a microcapsule suspension. For analysis, monolayers of dried capsules were prepared and agitated using a magnetic stir plate, and data was collected via microscopy with a confocal microscope and a USB microscope.

Data Analysis. Data was collected by videography for static and agitated microcapsule samples. Data analysis was performed using established image analysis techniques. Details of equipment are listed in the Supporting Information file.

RESULTS AND DISCUSSION

Density matching by the use of binary solvents is convenient as it gives an incredibly broad range of microparticle types that can be encapsulated. Density matching in combination with specific particle modifications has been shown in E-ink synthesis for Brownian scale microparticles.^{43–45}

If a particle adheres to the interface before membrane polymerization is sufficiently progressed, then it will become permanently embedded in the capsule wall. Therefore, the time taken for particles to reach the interface, t , must be more than the time taken for membrane formation. The time scale of mobility of Brownian or near-Brownian particles toward the interface can be described with the relationship $t \sim L^2/D$, where L is the distance of a particle from the interface and D is the particle diffusivity. Here, $D \propto r^{-1}$, where r is the particle radius (eq 1) and therefore the time taken to move to the interface, $t \propto r$.

$$D = \frac{kT}{6\pi\mu r} \quad (1)$$

However, as the particle size increases and buoyancy and sedimentation become more significant, the time for particles to reach the interface is inversely proportional to the settling velocity, v . As governed in eq 2, increasing the particle radius for a fixed particle density, ρ_p , and fluid viscosity, μ , will decrease t such that $t \propto r^{-2}$.

$$v = \frac{2(\rho_p - \rho_f)}{9} \frac{gr^2}{\mu} \quad (2)$$

As a result, the use of density matching, such that the density difference between the particles and the suspending fluid tends to zero, $(\rho_p - \rho_f) \rightarrow 0$, minimizes the buoyant and gravitational components of the particle motion, slowing particle transport toward the polymerizing interface, $t \propto 1/(\rho_p - \rho_f)$. Hence, the development of a typical polymeric encapsulation system utilizing both larger particles and density matching would be a synthetic approach with an inherent resistance to particle adsorption.

Providing that solvents are fully miscible, the density can be adjusted for any value between the density of solvent 1, ρ_1 , and solvent 2, ρ_2 . This is especially convenient when considering blends of materials such as low-density mineral oils and higher density halogenated oils, specifically those that are fluorinated.

Table 1. Composition of Components in the Microcapsule Samples

sample	$V_{\text{Binary}} [\text{cm}^3]$	$\phi_{p,\text{disp}}$	$m_{\text{particles}} [\text{g}]$	$m_{\text{span}} [\text{g}]$
0	7.5	0	0	0
1	7.5	2.5×10^{-3}	0.022	0.004
2	7.5	5.0×10^{-3}	0.044	0.009
3	7.5	7.5×10^{-3}	0.089	0.018
4	7.5	1.0×10^{-2}	0.273	0.055
5	7.5	3.0×10^{-2}	0.465	0.093
6	7.5	5.0×10^{-2}	0.717	0.144

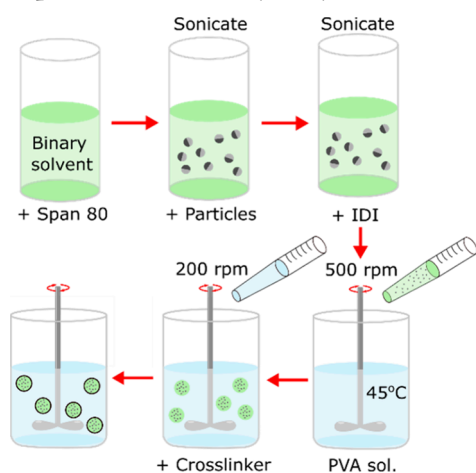
Here, a binary solvent system consisting of dodecane ($\rho_1 = 0.75 \text{ g cm}^{-3}$) and halocarbon 0.8 oil ($\rho_2 = 1.71 \text{ g cm}^{-3}$) was used. The halocarbon oils are a range of low molecular weight, oligomeric fluorinated oils based around polychlorotrifluoroethylene (PCTFE), with halocarbon 0.8 oil chosen due to its high density and low room temperature viscosity (0.8 cSt). [Figure S1, Supporting Information](#) shows the density curve for blends of dodecane and halocarbon oil, calculated volumetrically.

Poly(methyl methacrylate) (PMMA) particles with an approximate diameter of 35–55 μm ([Figures S2 and S3](#))⁴¹ were chosen due to their density ($\sim 1.18 \text{ g cm}^{-3}$), which lies within a density range (0.75–1.71 g cm^{-3}) that is easily adjusted for with conventional solvents. Provided that the density of a particle also lies within the same range, any large microparticle could be used. Referring back to the density curve, a solvent ratio of $\sim 2:1$ g:g of halocarbon:dodecane can be used to approximate density matched PMMA microparticles.

Magnetic Janus particles are used within this example of the synthesis as the particles can easily be manipulated by an external field to demonstrate that they are not adsorbed to the capsules' walls. The dual hemisphere nature of the particles highlights the translational and rotational freedom of the microparticles inside the microcapsules. A secondary advantage of using Janus particles is that they also demonstrate the robustness of this method toward microparticles with different surface chemistries. The specific particles here are half-coated with a thin 100 nm iron coating. This thin layer would only have a slight influence of the particle density ($< 0.02 \text{ g cm}^{-3}$) and was not included in the approximate particle density. A small amount of Span 80 was also used to reduce particle aggregation.⁴⁶

The synthetic method is shown in [Scheme 2](#) and discussed in the [Methods](#) section and [Table 1](#). The procedure follows a

Scheme 2. Scheme of the Reaction Process for Microencapsulation of Neutrally Buoyant Particles^a



^aGreen liquid indicates dispersed phase preparation, and blue represents the aqueous continuous phase.

simple emulsification of the dispersed phase containing the responsive particles. The reaction proceeds via an interfacial polymerization between oil-soluble isophorone diisocyanate (IDI) in the dispersed phase and water-soluble diethylene triamine (DETA) cross-linker added to the continuous phase, producing a polyurea capsule. The dispersed phase contains a volume fraction of Janus particles, $\phi_{p, \text{disp}}$, between 2.5×10^{-3} and 5.0×10^{-2} . The size distributions of the capsules are shown

in [Figure S4](#). The mean diameter of the capsules reduces, and the distribution narrows with increased $\phi_{p, \text{disp}}$ as the large particles increase the shear rate during emulsification. Capsule diameters range between ~ 450 and $265 \mu\text{m}$. The broad distributions are a result of the emulsification method. Additionally, during the synthesis, if the stir rate remains high after the addition of a cross-linker, then the capsules will be destroyed in the early stages of the reaction.

The synthesized capsules were exposed to an external actuating magnetic field (~ 1 to 8 mT) to assess the population of spatially manipulatable particles within each capsule. [Figure 1](#)

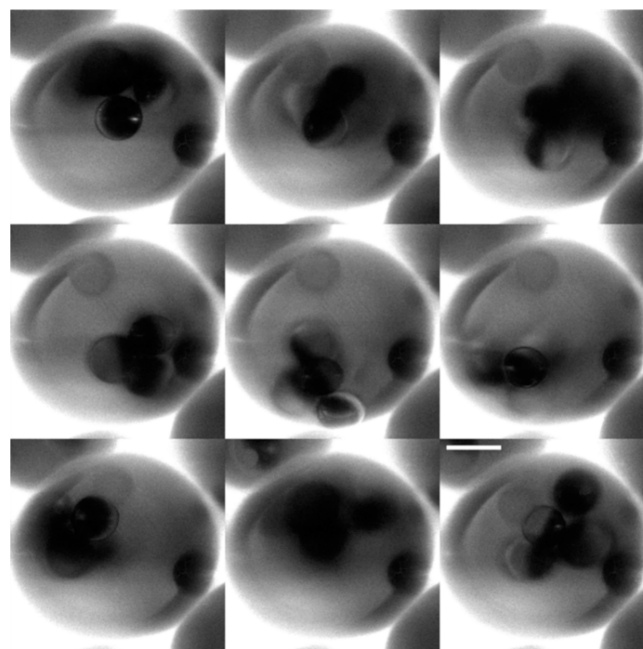


Figure 1. Montage of confocal microscopy images of a single microcapsule containing Janus particle suspension under agitation by an external field. Total duration = 4 s; images at 0.5 s intervals. Scale bar = 50 μm . $\phi_{p, \text{disp}} = 5.0 \times 10^{-2}$.

and [Movie S1](#) show a time-evolved image of a microcapsule containing Janus particles for a bulk particle concentration $\phi_{p, \text{disp}} = 5 \times 10^{-2}$. Over a 4 s period, particles are shown to freely rotate and translate throughout the core of the capsule. It should be noted that a particle embedded in the capsule wall will not be released by using a magnetic field. A lower magnification movie of a sample of $\phi_{p, \text{disp}} = 3.0 \times 10^{-2}$ is also shown in [Movie S2](#).

The number of particles per capsule, N_p , volume fraction of particles per capsule, $\phi_{p, \text{caps}}$, and fraction of mobile particles per capsule, Ω_p , are shown in [Table S1 of the Supporting Information](#), and results for Ω_p and $\phi_{p, \text{caps}}$ are represented in [Figure 2](#). Note that $\Omega_p = N_{\Omega, p} / N_{p, \text{total}}$ where $N_{\Omega, p}$ is the number of moving particles per capsule and $N_{p, \text{total}}$ is the total number of particles per capsule including those embedded in the membrane. As expected, N_p increases with increased $\phi_{p, \text{disp}}$ but begins to decrease at $\phi_{p, \text{caps}} = 5.0 \times 10^{-2}$ as the reducing average capsule size decreases the available space within capsules to hold particles. For $\phi_{p, \text{caps}}$ vs $\phi_{p, \text{disp}}$, initially, the slope of the trend is > 1 , suggesting that the tendency of particles to dimerize or chain locally increases the particle concentration for some droplets during emulsification. From $\phi_{p, \text{disp}} = 1.0 \times 10^{-2}$ onward, the slope is < 1 , suggesting that a fraction of particles are being lost to the aqueous phase during emulsification,

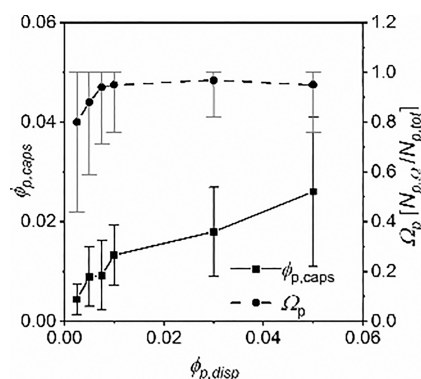


Figure 2. (Black line, black squares) Volume fraction of magnetic particles inside capsules, $\phi_{p,caps}$ against the initial dispersed phase volume fraction, $\phi_{p,disp}$. (Dash line, black circles) Fraction of particles within a capsule, which move under applied field manipulation, Ω_p . Measurements were taken per capsule for a minimum of 300 capsules.

indicating a decreased efficiency in the encapsulation process, possibly due to droplet overcrowding or enlarged cluster sizes. As $\phi_{p,disp}$ increases, the fraction of mobile particles per capsule, Ω_p , increases to close to 1 as the statistical significance of capsules containing single immobile particles is nullified. For this system, trends suggest an optimal synthesis at $\phi_{p,disp} \approx 2.0 \times 10^{-2}$ where the $\phi_{p,disp} \approx \phi_{p,caps}$, which also coincides well with close to $\Omega_{p,max}$. From a global perspective, for a different particle-capsule system, the results suggest an optimization based on capsule overcrowding and optimal $\phi_{p,caps}$.

This synthetic technique has also been effective for smaller particle sizes, such as 3, 5, and 8 μm polystyrene particles and also 9–13 μm glass particles and nickel flakes. However, there is visibly reduced encapsulation efficacy and Ω_p for smaller particle sizes ($d \leq 2 \mu\text{m}$) where Brownian motion plays a more significant role.

To demonstrate the utility of this synthetic method to general applications, we can utilize one of the inherent properties of Janus particle suspensions, as shown previously by Gao et al.⁴⁷ Janus particle suspensions show an optical dynamic range, depending on their orientation and degree of chaining. Among the many possible applications discussed in the **Introduction**, one which is particularly applicable to this observation is magnetically actuated display materials. Other work also discusses the optical dynamic range of suspensions of suspended magnetic particles.⁴⁸ Specifically, for the work of Gao and co-workers, the orientation of assembled Janus particle chains and clusters relative to an applied magnetic field gives rise to variable transmission of light, essentially as a consequence of the projected surface area of assembled particles. The use of larger Janus particles was also shown to be useful in screen-like devices, though these approaches did not involve microencapsulation.^{49–51} Compartmentalization of these particle suspensions produces microcapsules that display the same optical dynamic properties. The advantages here would be the lack of requirement for a transparent electrode, thus reducing device expense and fragility, yet also giving an order of magnitude increase in the refresh rate of rotating magnetic particles compared to translational motion of particles, such as those seen in established E-inks.⁴³ **Figure 3** shows the results of the analysis of relative intensity difference of these microcapsules at different $\phi_{p,disp}$ as they are subjected to a variable magnetic field, but an example of the macroscopic phenomenon can be seen in **Movie S3**. **Figure 3A** shows the relative intensity difference for capsules

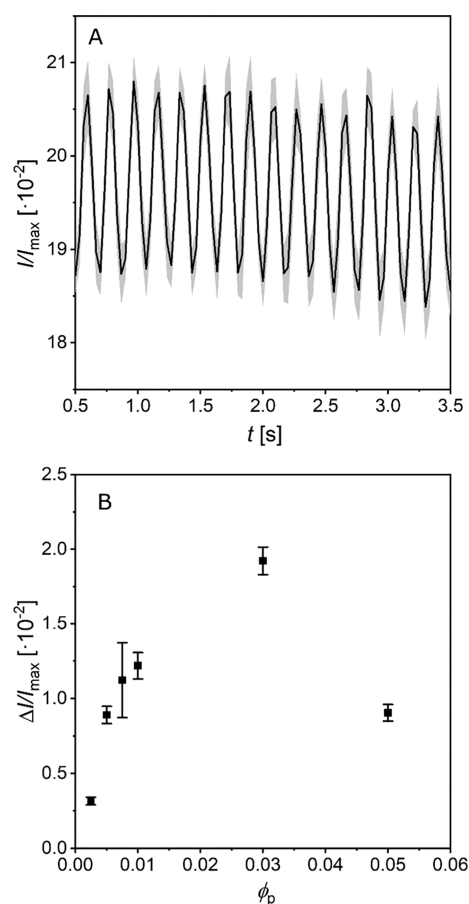


Figure 3. (A) Relative intensity difference of capsules in a rotating magnetic field for a $\phi_{p,disp} = 3.0 \times 10^{-2}$. (B) $\Delta I/I_{max}$ for capsules prepared from dispersed phases with increasing $\phi_{p,disp}$.

prepared from $\phi_{p,disp} = 3.0 \times 10^{-2}$ for a magnetic field changing at a frequency of ~ 4.8 Hz. **Figure 3B** shows the difference between I_{min} and I_{max} over every magnetic pole switch, averaged over 4 s for each $\phi_{p,disp}$. The measured intensity difference is in the range of 0.31–1.92% and is comparable to that shown in a previous study with smaller particles.²⁴ This range depends on several material parameters that remain far from being optimized in this study. The trend in $\Delta I/I_{max}$ increases with $\phi_{p,disp}$ up to 3.0×10^{-2} , which is comparable to the synthetic optimization discussed earlier. $\Delta I/I_{max}$ then decreases. This can be explained in two ways. First, as discussed, the orientation of Janus particles is the phenomenon that produces the intensity difference through the changing projected surface area of particles, particle chains, and particle clusters, which in turn changes the transmission/reflection of light through a capsule. As $\phi_{p,caps}$ increases, the particles are covering an increasing projected surface area. There will be a critical $\phi_{p,caps}$ at which $\Delta I/I_{max}$ is optimized. At concentrations higher than this, overcrowding inside capsules and particles lost into the aqueous phase remains in the dried samples preventing passage of light through the samples, and $\Delta I/I_{max}$ reduces. Second, overcrowding in capsules can disrupt capsule membrane formation. This results in capsule surface defects, which affect the refractive index difference of the capsule membranes, leading to a slight loss of transparency in the visible range. These are two mechanisms that can be optimized by altering particle size, reflectivity and absorbance, volume fraction, and the background and lighting used.

CONCLUSIONS

In conclusion, density matching of non-Brownian microparticles with a binary dispersed phase has been shown to be an effective route to microencapsulation of microparticles, importantly with a high percentage of particles remaining mobile within the capsule cores when exposed to an external stimulus. The method is also seen to be resistant to particles that have complex/asymmetric wetting properties. The general utility of the method is demonstrated by incorporating magneto-responsive Janus particles inside the cores of the capsules. The aim is to retain the previously reported optical properties of Janus particle suspensions after microencapsulation. When exposed to a variable magnetic field, the relative transmission of light through the sample oscillates in accordance with findings from the literature but is importantly a visually tangible demonstration of the retention of particle mobility within the capsules without modification of the suspending fluid rheology. The optimal synthetic procedure for maximizing microparticle mobility is comparable to the optimized procedure found for preserving optical activity, showing the robustness of this general procedure.

ASSOCIATED CONTENT

Supporting Information

The Supporting Information is available free of charge at <https://pubs.acs.org/doi/10.1021/acs.jpcb.4c02288>.

Information regarding equipment and materials, particle characterization, and additional capsule characterization (PDF)

Movie 1: Counterpart movie to Figure 1, confocal microscopy recording of particles being agitated inside the core of a capsule (AVI)

Movie 2: Low magnification recording of capsules containing particles under magnetic agitation (AVI)

Movie 3: Macroscopic recording of slurry of wet capsules demonstrating variable optical properties under magnetic agitation (AVI)

AUTHOR INFORMATION

Corresponding Authors

Samuel R. Wilson-Whitford – School of Engineering, The University of Warwick, Coventry CV4 7AL, U.K.;

ORCID: orcid.org/0000-0001-6065-8451; Email: samuel.wilson-whitford@warwick.ac.uk

James F. Gilchrist – Department of Chemical and Biomolecular Engineering, Lehigh University, Bethlehem, Pennsylvania 18015, United States; ORCID: orcid.org/0000-0003-2066-750X; Email: gilchrist@lehigh.edu

Author

Jinghui Gao – Department of Chemical and Biomolecular Engineering, Lehigh University, Bethlehem, Pennsylvania 18015, United States

Complete contact information is available at: <https://pubs.acs.org/doi/10.1021/acs.jpcb.4c02288>

Author Contributions

S.R.W.-W. contributed to the conceptualization, experimentation, data analysis, drafting, and editing of the manuscript. J.G. contributed to the experimentation. J.F.G. contributed to the conceptualization and editing of the manuscript.

Funding

Funding for this work was provided by the Applied Physics Laboratory, Johns Hopkins University.

Notes

The authors declare no competing financial interest.

REFERENCES

- (1) Subramaniam, A. B.; Abkarian, M.; Stone, H. A. Controlling Assembly of Jammed Colloidal Shells on Fluid Droplets. *Nat. Mater.* **2005**, *4*, 553–556.
- (2) Jaggars, R. W.; Chen, R.; Bon, S. A. F. Control of Vesicle Membrane Permeability with Catalytic Particles. *Mater. Horiz.* **2016**, *3*, 41–46.
- (3) Hamad, S. A.; Stoyanov, D.; Paunov, V. N. Triggered Cell Release from Shellac-Cell Composite Microcapsules. *Soft Matter* **2012**, *8*, 5069–5077.
- (4) Sander, J. S.; Studart, A. R. Monodisperse Functional Colloidosomes with Tailored Nanoparticle Shells. *Langmuir* **2011**, *27*, 3301–3307.
- (5) Yin, Y.; Zeng, X.; Liu, W.; Xue, Y.; Li, X.; Wang, W.; Song, Y.; Zhu, Z.; Yang, C. Stable Colloidosomes Formed by Self-Assembly of Colloidal Surfactant for Highly Robust Digital PCR. *Anal. Chem.* **2019**, *91*, 6003–6011.
- (6) Liu, Z.; Wang, B.; Jin, S.; Wang, Z.; Wang, L.; Liang, S. Bioinspired Dual-Enzyme Colloidosome Reactors for High-Performance Biphasic Catalysis. *ACS Appl. Mater. Interfaces* **2018**, *10*, 41504–41511.
- (7) Welling, T. A. J.; Watanabe, K.; Grau-Carbonell, A.; De Graaf, J.; Nagao, D.; Imhof, A.; Van Huis, M. A.; Van Blaaderen, A. Tunability of Interactions between the Core and Shell in Rattle-Type Particles Studied with Liquid-Cell Electron Microscopy. *ACS Nano* **2021**, *15*, 11137–11149.
- (8) Kim, H.; Fortunato, M. E.; Xu, H.; Bang, J. H.; Suslick, K. S. Carbon Microspheres as Supercapacitors. *J. Phys. Chem. C* **2011**, *115*, 20481–20486.
- (9) Qiao, Z.-A.; Guo, B.; Binder, A. J.; Chen, J.; Veith, G. M.; Dai, S. Controlled Synthesis of Mesoporous Carbon Nanostructures via a “Silica-Assisted” Strategy. *Nano Lett.* **2013**, *13*, 207–212.
- (10) Yang, Z.; Li, M.; Zhang, Y.; Yang, L.; Liu, J.; Wang, Y.; He, Q. Constructing Uniform Fe₃O₄@C@MnO₂ Microspheres with Yolk-Shell Interior Towards Enhancement in Microwave Absorption. *J. Alloys Compd.* **2020**, *817*, No. 152795.
- (11) Pickering, S. U. Emulsions. *J. Chem. Soc., Trans.* **1907**, *91*, 2001–2021.
- (12) Ramsden, W. Separation of solids in the surface-layers of solutions and ‘suspensions’ (observations on surface-membranes, bubbles, emulsions, and mechanical coagulation).—Preliminary account. *Proc. R. Soc. London* **1904**, *72*, 156–164.
- (13) Finkle, P.; Draper, H. D.; Hildebrand, J. H. The Theory of Emulsification. *J. Am. Chem. Soc.* **1923**, *45*, 2780–2788.
- (14) Pieranski, P. Two-Dimensional Interfacial Colloidal Crystals. *Phys. Rev. Lett.* **1980**, *45*, 569–572.
- (15) Aveyard, R.; Clint, J. H. Particle Wettability and Line Tension. *J. Chem. Soc. - Faraday Trans.* **1996**, *92*, 85–89.
- (16) Nie, Z.; Park, J. I.; Li, W.; Bon, S. A. F.; Kumacheva, E. An “Inside-Out” Microfluidic Approach to Monodisperse Emulsions Stabilized by Solid Particles. *J. Am. Chem. Soc.* **2008**, *130*, 16508–16509.
- (17) Castellanos, N. I.; Bharti, B.; Velev, O. D. Field-Driven Reversible Alignment and Gelation of Magneto-Responsive Soft Anisotropic Microbeads. *J. Phys. Chem. B* **2021**, *125*, 7900–7910.
- (18) Seeto, W. J.; Tian, Y.; Pradhan, S.; Kersch, P.; Lipke, E. A. Rapid Production of Cell-Laden Microspheres Using a Flexible Microfluidic Encapsulation Platform. *Small* **2019**, *15*, 1902058.
- (19) Ge, J.; Lee, H.; He, L.; Kim, J.; Lu, Z.; Kim, H.; Goebel, J.; Kwon, S.; Yin, Y. Magneto-chromic Microspheres: optating Photonic Crystals. *J. Am. Chem. Soc.* **2009**, *131*, 15687–15694.

- (20) Dyab, A. K. F.; Ozmen, M.; Ersoz, M.; Paunov, V. N. Fabrication of Novel Anisotropic Magnetic Microparticles. *J. Mater. Chem.* **2009**, *19*, 3475–3481.
- (21) Lim, F. Preparation of Substances with Encapsulated Cells. US4409331A, 1983.
- (22) Lim, F. Encapsulation of Biological Material. US4352883A, 1982.
- (23) Lim, F.; Moss, R. D. Microencapsulation of Living Cells and Tissues. *J. Pharm. Sci.* **1981**, *70*, 351–354.
- (24) Wilson-Whitford, S. R.; Gao, J.; Roffin, M. C.; Kaewpetch, T.; Gilchrist, J. F. Yield Stress-Enabled Microencapsulation of Field-Responsive Microparticle Suspensions. *Soft Matter* **2023**, *19*, 9139–9145.
- (25) Suzuki, T.; Osumi, A.; Minami, H. One-Step Synthesis of “Rattle-Like” Polymer Particles via Suspension Polymerisation. *Chem. Commun.* **2014**, *50*, 9921–9924.
- (26) Zou, S.; Hu, Y.; Wang, C. One-Pot Fabrication of Rattle-Like Capsules with Multicores by Pickering-Based Polymerization with Nanoparticle Nucleation. *Macromol. Rapid Commun.* **2014**, *35*, 1414–1418.
- (27) Wang, Z.; Qiu, T.; Guo, L.; Ye, J.; He, L.; Li, X. Polymerization induced shaping of Pickering emulsion droplets: From simple hollow microspheres to molecularly imprinted multicore microrattles. *Chem. Eng. J.* **2018**, *332*, 409–418.
- (28) Zhang, M.; Lan, Y.; Wang, D.; Yan, R.; Wang, S.; Yang, L.; Zhang, W. Synthesis of Polymeric Yolk-Shell Microspheres by Seed Emulsion Polymerization. *Macromolecules* **2011**, *44*, 842–847.
- (29) Wang, J.; Yang, Z.; Xu, J.; Ahmad, M.; Zhang, H.; Zhang, A.; Zhang, Q.; Kou, X.; Zhang, Q. Surface Microstructure Regulation of Porous Polymer Microspheres by Volume Contraction of Phase Separation Process in Traditional Suspension Polymerization System. *Macromol. Rapid Commun.* **2019**, *40*, 1800768.
- (30) Li, H.; Bian, Z.; Zhu, J.; Zhang, D.; Li, G.; Huo, Y.; Li, H.; Lu, Y. Mesoporous Titania Spheres with Tunable Chamber Structure and Enhanced Photocatalytic activity. *J. Am. Chem. Soc.* **2007**, *129*, 8406–8407.
- (31) Liu, S.; Xia, J.; Yu, J. Amine-Functionalized Titanate Nanosheet-Assembled Yolk@Shell Microspheres for Efficient Cocatalyst-Free Visible-Light Photocatalytic CO₂ Reduction. *ACS Appl. Mater. Interfaces* **2015**, *7*, 8166–8175.
- (32) Watanabe, K.; Ishii, H.; Konno, M.; Imhof, A.; Van Blaaderen, A.; Nagao, D. Yolk/Shell Colloidal Crystals Incorporating Movable Cores with Their Motion Controlled by an External Electric Field. *Langmuir* **2017**, *33*, 296–302.
- (33) Nagao, D.; Van Kats, C. M.; Hayasaka, K.; Sugimoto, M.; Konno, M.; Imhof, A.; Van Blaaderen, A. Synthesis of Hollow Asymmetrical Silica Dumbbells with a Moveable Inner Core. *Langmuir* **2010**, *26*, 5208–5212.
- (34) Okada, A.; Nagao, D.; Ueno, T.; Ishii, H.; Konno, M. Colloidal Polarization of Yolk/Shell Particles by Reconfiguration of Inner Cores Responsive to an External Magnetic Field. *Langmuir* **2013**, *29*, 9004–9009.
- (35) Watanabe, K.; Nagao, D.; Ishii, H.; Konno, M. Rattle-Type Colloidal Crystals Composed of Spherical Hollow Particles Containing an Anisotropic, Movable Core. *Langmuir* **2015**, *31*, 5306–5310.
- (36) Liu, Z.; Zhao, Y.; He, R.; Luo, W.; Meng, J.; Yu, Q.; Zhao, D.; Zhou, L.; Mai, L. Yolk@Shell SiO₂/C Microspheres with Semi-Graphitic Carbon Coating on the Exterior and Interior Surfaces for Durable Lithium Storage. *Energy Storage Mater.* **2019**, *19*, 299–305.
- (37) Yoo, J. B.; Yoo, H. J.; Lim, B. W.; Lee, K. H.; Kim, M. H.; Kang, D.; Hur, N. H. Controlled Synthesis of Monodisperse SiO₂-TiO₂ Microspheres with a Yolk-Shell Structure as Effective Photocatalysts. *ChemSusChem* **2012**, *5*, 2334–2340.
- (38) Caruso, M. M.; Schelkopf, S. R.; Jackson, A. C.; Landry, A. M.; Braun, P. V.; Moore, J. S. Microcapsules Containing Suspensions of Carbon Nanotubes. *J. Mater. Chem.* **2009**, *19*, 6093–6096.
- (39) Guo, H.; Zhao, X.; Wang, J. Synthesis of Functional Microcapsules Containing Suspensions Responsive to Electric Fields. *J. Colloid Interface Sci.* **2005**, *284*, 646–651.
- (40) Klein, S. M.; Manoharan, V. N.; Pine, D. J.; Lange, F. F. Synthesis of Spherical Polymer and Titania Photonic Crystallites. *Langmuir* **2005**, *21*, 6669–6674.
- (41) Wilson-Whitford, S. R.; Gao, J.; Roffin, M. C.; Buckley, W. E.; Gilchrist, J. F. Microrollers Flow Uphill as Granular Media. *Nat. Commun.* **2023**, *14*, 5829.
- (42) Li, X.; Gilchrist, J. F. Large-Area Nanoparticle Films by Continuous Automated Langmuir-Blodgett Assembly and Deposition. *Langmuir* **2016**, *32*, 1220–1226.
- (43) Comiskey, B.; Albert, J. D.; Yoshizawa, H.; Jacobson, J. An Electrophoretic Ink for All-Printed Reflective Electronic Displays. *Nature* **1998**, *394*, 253–255.
- (44) Yu, D. G.; Kim, S. H.; An, J. H. Preparation and Characterization of Electronic Inks Encapsulation for Microcapsule-Type Electrophoretic Displays (EPDs). *J. Ind. Eng. Chem.* **2007**, *13*, 438–443.
- (45) Wang, Y. T.; Zhao, X. P.; Wang, D. W. Electrophoretic Ink Using Urea-Formaldehyde Microspheres. *J. Microencapsul.* **2006**, *23*, 762–768.
- (46) Smith, G. N.; Eastoe, J. Controlling Colloid Charge in Nonpolar Liquids with Surfactants. *Phys. Chem. Chem. Phys.* **2013**, *15*, 424–439.
- (47) Gao, J.; Wilson-Whitford, S. R.; Han, S. E.; Han, S. M.; Gilchrist, J. F. Dynamic Emissivity of Self-Assembled Magnetoresponse Janus Particle Chain Suspensions. *ACS Appl. Opt. Mater.* **2023**, *1* (1), 430–434.
- (48) Martin, J. E.; Hill, K. M.; Tigges, C. P. Magnetic-Field-Induced Optical Transmittance in Colloidal Suspensions. *Phys. Rev. E* **1999**, *59*, 5676–5692.
- (49) Nisisako, T.; Torii, T.; Takahashi, T.; Takizawa, Y. Synthesis of Monodisperse Bicolored Janus Particles with Electrical Anisotropy Using a Microfluidic Co-Flow System. *Adv. Mater.* **2006**, *18*, 1152–1156.
- (50) Komazaki, Y.; Hirama, H.; Torii, T. Electrically and Magnetically Dual-Driven Janus Particles for Handwriting-Enabled Electronic Paper. *J. Appl. Phys.* **2015**, *117*, 154506.
- (51) Yin, S.-N.; Wang, C.-F.; Yu, Z.-Y.; Wang, J.; Liu, S.-S.; Chen, S. Versatile Bifunctional Magnetic-Fluorescent Responsive Janus Supraballs Towards the Flexible Bead Display. *Adv. Mater.* **2011**, *23*, 2915–2919.